# Determination of low level of actinium 227 in seawater and freshwater by isotope dilution and mass spectrometry

M. Levier, M. Roy-Barman, C. Colin, A. Dapoigny

# Determination of low level of actinium 227 in seawater and freshwater by isotope dilution and mass spectrometry

M. Levier[1], M. Roy-Barman[1], C. Colin[2], A. Dapoigny[1]

[1]Université Paris-Saclay, CNRS, CEA, UVSQ, Laboratoire des Sciences du Climat et de l'Environnement, 91191 Gif-sur-Yvette, France,
martin.levier@lsce.ipsl.fr, matthieu.roy-barman@lsce.ipsl.fr, arnaud.dapoigny@lsce.ipsl.fr

[2]Université Paris-Saclay, CNRS, GEOPS, 91405, Orsay, France,
christophe.colin@universite-paris-saclay.fr

Abstract :

By diffusing from the sediments into the ocean, $^{227}$Ac (half-life = 21.7 y) is a powerful tracer of vertical mixing in the deep ocean on decadal time scales. However, its use is limited by its very low concentration resulting in large volumes (hundreds of L) of water required for its analysis. We have developed a new method of $^{227}$Ac analysis by isotope dilution and MC-ICPMS that significantly improves the measurement accuracy and reduces the sample size (10-30 L). After spiking water samples with $^{225}$Ac milked from a $^{229}$Th solution, actinium isotopes are preconcentrated by manganese co-precipitation, purified by chromatographic methods and then measured by MC-ICPMS. The performance of the analytical method (accuracy, precision) was estimated with a homemade actinium standard solution. An internal quality control was carried out to validate the method by repeated measurements of 2 L of surface seawater doped with $^{227}$Ac (1000 ag/kg) and duplicates of the Vienne river water (6.1 ± 1.7 ag/kg and 4.1 ± 1.3 ag/kg). $^{231}$Pa was also co-precipitated, purified during the chromatography and analysed by MC-ICPMS. The combined measurement of $^{227}$Ac and $^{231}$Pa from the same sample allows discriminating $^{227}$Ac supported by $^{231}$Pa decay from the $^{227}$Ac released by remobilization from the sediments. The $^{227}$Ac concentrations measured on the first seawater samples of 29 L from the South China Sea water range from below the detection limit in surface water (~ 0.5 ag/kg for 30 L) to 3.4 ± 0.5 ag/kg at 2760 m depth (uncertainties are given in $2\sigma_n$). The $^{227}$Ac measured in the deep South China Sea waters entering through the Luzon strait are consistent with previous data obtained in the same water mass in the Pacific Ocean (PDW). Seawater from the southernmost station of Bonus GoodHope, in the Weddell Gyre, were also analysed, with $^{227}$Ac concentration ranging from 4.2 ± 0.4 ag/kg to 10.9 ± 1.0 ag/kg in good agreement with previous measurement in the Weddell Gyre by Geibert et al. (2002, 2008).

## 1. Introduction

Natural radioelements of the uranium decay and thorium chains are recognized chronometers of ocean processes. $^{227}$Ac (half-life = 21.8 y) is produced by radioactive decay of $^{231}$Pa (half-life =32400 y), its precursor in the $^{235}$U decay chain. In the ocean, highly insoluble $^{231}$Pa is scavenged by marine particles and transported to the seafloor where it decays to $^{227}$Ac. Then soluble $^{227}$Ac is released to the bottom water where it becomes a chronometer of the vertical eddy diffusion (Nozaki, 1993, 1984). The $^{231}$Pa of seawater must be determined to calculate the excess of $^{227}$Ac ($^{227}Ac_{ex}$) compared to the $^{227}$Ac expected at the equilibrium with $^{231}$Pa (also called supported $^{227}$Ac). However, $^{227}$Ac measurement is rarely used in oceanographic studies due to its very low concentration in seawater: from 0.5 ag/kg to 30 ag/kg (1 ag/kg = $10^{-18}$ g/L; 1 dpm/m$^3$ = 6.23 ag/kg) and the need for large seawater volumes that are needed to perform each measurement, limiting the use of this tracer. Initially, $^{227}$Ac measurements were made by alpha-spectrometry after processing of several hundred litres of seawater (Geibert et al., 2002; Nozaki, 1984). Subsequent developments on alpha spectrometry allowed (1) reducing sample size below 100 litres and (2) using $^{225}$Ac as yield tracer (Bojanowski et al., 1987; Geibert and Vöge, 2008). Recently, $^{227}$Ac analysis by Radium Delay Coincidence Counting (RaDeCC) was introduced, with actinium being concentrated on cartridges with *in situ* pump, requiring thousands litres of seawater (Le Roy et al., 2019; Shaw and Moore, 2002, Kipp et al, 2015). Since then, RaDeCC has become the only method used to analyse $^{227}$Ac in seawater within the GEOTRACES international program (Geibert, 2015). However, aside from the large volume requirements, RaDeCC brings also large analytical uncertainties due to poor counting statistics and to uncertainty of the preconcentration yield. Also, RaDeCC does not allow determination of the $^{231}$Pa concentration.

Recently, the analysis of $^{227}$Ac by isotope dilution (ID) and MultiCollector Induced Coupled Plasma mass spectrometry (MC-ICPMS) was developed for nuclear forensic applications (Kayzar and Williams, 2015). This method was applied to $^{227}$Ac-rich samples (uranium oxide, geological samples) typically allowing the analysis of around 100000 ag of $^{227}$Ac, which is a factor 200 to 5000 more than what we can expect in ~10-30 L of seawater. Recent developments made at LSCE allow us to measure quantities as low as 0.1 fg (100 ag) of $^{231}$Pa by MC-ICPMS (Gdaniec et al., 2020; Roy-Barman et al., 2020), a level comparable to the $^{227}$Ac content of a few tens of litres of deep seawater. In the present work, we build on Kayzar and Williams (2015) to propose a new protocol to pre-concentrate and purify $^{227}$Ac from 10-30 L of seawater or continental water and analyse it by isotopic dilution and MC-ICPMS, with a precision at least equivalent to the alpha counting or RaDeCC.

## 2. Methods

### 1. Standards, spike and samples

All reagents were prepared with Normatom™ trace element analytical grade acids and 18.2 MΩ MilliQ™ water.

Several uranium and thorium solutions and an uraninite powder were used as sources of actinium isotopes and references for concentration calibration during the course of this work.

*$^{229}$Th and $^{225}$Ac spikes*: a $^{229}$Th spike solution from Eckert and Ziegler ($^{229}$Th concentration ≈1 ng/g) was used as source of $^{225}$Ac spike. At secular equilibrium, 1.0 ng of $^{229}$Th (half-life = 7917 y, Varga et al., 2014) is at equilibrium with 3370 ag of $^{225}$Ac (half-life = 9.92 d, Pommé et al., 2012). This $^{229}$Th spike was calibrated against a $^{232}$Th standard described below.

87 *$^{232}$Th standard*: a $^{232}$Th (+ $^{230}$Th) in-house standard solution was used to calibrate the $^{229}$Th
88 spike. The concentration of this $^{232}$Th standard is relatively well known. It is used at LSCE as
89 reference to calibrate new $^{229}$Th spikes solutions for seawater analysis, in particular during the
90 GEOTRACES intercalibration process (Anderson et al., 2012, Gdaniec et al., in prep.).
91 Therefore, we consider that we know its concentration with an expanded uncertainty within 1
92 or 2%.

93 *Harwell Uraninite*: We used the Harwell Uraninite (HU1) that is known to be at secular
94 equilibrium for the $^{235}$U decay chain (Komura et al., 1990) to prepare a purified $^{227}$Ac
95 solution.

96 Moreover, different samples artificially enriched in $^{227}$Ac were prepared to test the method:

97 - *Artificial seawaters enriched in $^{227}$Ac* (hereafter referred to as "Artificial seawaters ") were
98 prepared by dissolving 8.75 g of NaCl in 250mL of water, and adding 200 ng of Re
99 (equivalent Re in 10~30 L of seawater). These artificial seawaters were then enriched by
100 adding 2000 ag of $^{227}$Ac (grossly the $^{227}$Ac amount expected in 30 L of deep water) from our
101 stock solution.

102 - *surface Mediterranean water enriched in $^{227}$Ac* (hereafter referred to as "enriched
103 Mediterranean seawater ") were also prepared by adding 2000 ag of $^{227}$Ac to 2 L of surface
104 seawater (depth = 60 m) collected in the Sicily Strait. Due to very low $^{231}$Pa content of this
105 water (Gdaniec et al., 2018), the contribution of $^{227}$Ac initially present in the sample was less
106 than 0.2% of the added $^{227}$Ac ($^{227}$Ac in this surface water = 2 ag/kg).

107

108 Different water samples were collected to test the analytical procedure:

- freshwater from the Vienne river (46°24.25'N, 0°42.12'E), a river draining a strongly granitic watershed;

- freshwater from the "mare du Rusquec", a small pond in Britany (France, 48°19.68'N, 3°48.63'W), where very high $^{227}$Ac concentrations in the pond sediments have been observed previously;

- seawater from a vertical profile in the South China Sea (21°26.49'N, 120°12.57'E) collected during the HYDROSED cruise in June 2018. All the samples were filtered on board using AcroPak 500 capsule filter (porosity: 0.8-0.45µm) before being acidified to pH<2 with ultra-pure 6M hydrochloric acid. HYDROSED seawater samples were sub-sampled to measure Pa and Th independently with 4 L.

- Seawater samples from the Atlantic sector of the southern Ocean (57°55'S, 00°03'W) were collected during the Bonus GoodHope cruise in 2008 (Roy-Barman et al., 2019). They were filtered (Nuclepore, 90mm diameter, 0.4 µm pore size) and acidified on board (pH = 2).

## 2. Chemical protocols

We developed several protocols:

(1) to prepare a $^{227}$Ac standard from an uraninite powder,

(2) to calibrate the $^{227}$Ac with a $^{229}$Th spike at secular equilibrium with $^{225}$Ac,

(3) to extract $^{225}$Ac by "milking" of a $^{229}$Th source to avoid using large quantities of $^{229}$Th for sample analysis (both for saving spike and for safety purpose),

(4) finally, to preconcentrate and purify Ac from natural water samples.

### a. $^{227}$Ac standard preparation

We prepared a $^{227}Ac$ stock solution by extracting and purifying $^{227}Ac$ from the HU1 uraninite. 200 mg of HU1 powder were dissolved in 8M $HNO_3$. $^{227}Ac$ was then separated by chromatographic methods. The first column (Triskem, 0.67 cm, h = 6 cm) was filled with 2 mL of anion exchange resin Dowex AG1x8 200-400 mesh (Gdaniec et al., 2020, 2018). To prevent the resin saturation by U, we split the dissolved uraninite into four columns eluted simultaneously in parallel. We extracted three fractions: first, thorium (Th), radium (Ra) and actinium (Ac) were eluted with 10 mL 9M HCl, then protactinium (Pa) was eluted with 10mL 9M HCl + 0.1M HF and finally, uranium (U) was recovered eluted with 6 mL of MilliQ water. The Ac-Th-Ra fraction was evaporated on a hotplate and then dissolved in 4M $HNO_3$. A second column was used to separate Ac from Ra and Rare Earth Elements (REE) which could produce isobaric interferences during the measurement by MC-ICPMS (see measurement section). This second column was filled with 1 mL (⌀= 0.67 cm, h=3cm) of an extraction resin: the Triskem TODGA 200-400 mesh resin (Kayzar and Williams, 2015; Marinov et al., 2016; Radchenko et al., 2015). First, Ra was eluted with 15 mL 4M $HNO_3$. Then, purified Ac was recovered with 30mL of 10M $HNO_3$. The $^{227}Ac$ stock was diluted to a concentration close to 10 fg/g.

b. Calibration of the $^{227}Ac$ standard

The $^{227}Ac$ stock solution concentration needed to be calibrated because the yield of the procedure described in the previous section may not be 100%. Around 2000 ag of $^{227}Ac$ were used to calibrate the concentration of the stock solution. The calibration was made by isotopic dilution by adding 1 ng of $^{229}Th$ at equilibrium with $^{225}Ac$. We separated actinium from the thorium with a 1 mL TODGA column. The $^{225}Ra$ was eluted with 15 mL of 4M $HNO_3$ and then actinium isotopes were eluted with 30 mL 10M $HNO_3$. The actinium fraction was

155 evaporated and dissolved in 1M $HNO_3$ + 0.013M HF. The solution was filtered at 0.4 µm to
156 remove any resin grain before analysis by MC-ICPMS.

157 c. Milking $^{225}Ac$

158 A purified $^{225}Ac$ spike was used for the actinium analysis in seawater samples by isotopic
159 dilution. The spike was produced by milking $^{225}Ac$ from 8 ng of a $^{229}Th$ solution. The
160 separation of $^{225}Ac$ from $^{229}Th$ and $^{225}Ra$ was done through a chromatographic column
161 (Triskem TODGA 1 mL). Radium was eluted with 15 mL of 4M $HNO_3$ (no Ra sorption in
162 nitric acid on TODGA, while Ac $K_d$ is 1000), the actinium was eluted with 30 mL of 10M
163 $HNO_3$ (Radchenko et al., 2015). Thorium has a very strong affinity for the TODGA resin ($K_d$
164 > $10^4$, Pourmand and Dauphas, 2010), so the $^{229}Th$ cow is stored directly on the column until
165 the next milking. For this purpose, the column was filled with 4M $HNO_3$ and tightly closed to
166 avoid the drying of the resin.

167

168 d. Artificial and natural water processing

169 Analysing 10-30L seawater samples required to pre-concentrate $^{227}Ac$ through an iron or
170 manganese coprecipitation step. The different iron solutions used for our initial tests of co-
171 precipitation brought around 250 cps of isobaric interferences on the masses 225 and 227. Co-
172 precipitation tests made with manganese revealed no obvious interferences. Therefore,
173 manganese was selected. We tested every other reagent of the chemistry to estimate their
174 contribution to interferences.

175 To process samples, we added around 1000 ag of milked $^{225}Ac$ and around 3 fg of $^{233}Pa$ to
176 each sample. The relatively large amount of $^{225}Ac$ used here took into account its decay
177 during the 2-3 week's duration of the protocol. We carried out a manganese oxide

coprecipitation by adjusting the pH to 8-9 and adding 9 mg of $KMnO_4$ (300 µL of 30 g/L $KMnO_4$ solution) and 24 mg of $MnCl_2$ (240 µL of 100 g/L $MnCl_2$ solution). We let the reaction occur for at least 8 hours (Ghaleb et al., 2004; Rutgers van der Loeff and Moore, 1999). When the water processed had a high dissolved silica content (eg; deep Pacific waters), $MnO_2$ precipitation also produced silica gel formation (Gdaniec et al., 2017). The Mn oxides (and silica gel) were recovered by filtration on a Nuclepore$^{TM}$ filter (diameter: 142 mm, pore size: 0.45µm, nitrocellulose. The precipitate was rinsed on the filter with at least 2L of MQ to leach out major elements as Na and Ca from the precipitate. We dissolved the Mn oxide from the filter in a bath of 75mL of 6 M HCl with 100 µL of $H_2O_2$ and 100 µL of 27M HF during 30 min. After manganese oxides dissolution, the filter was rinsed with 6M HCl. The dissolution bath was evaporated to dryness and the residue dissolved in 10 mL of HCl, 6M. This silica gel was separated from the solution by centrifugation (5 min at 4000 rpm). After removal of the supernatant, the silica gel "sink" was washed with 6M HCl and separated again by centrifugation before dissolution with 100µL of 27M HF. The solution was dried and dissolved with 80 µL of 12M HCl saturated with boric acid. The resulting solution was added to the supernatants to be dried and dissolved in 9M HCl.

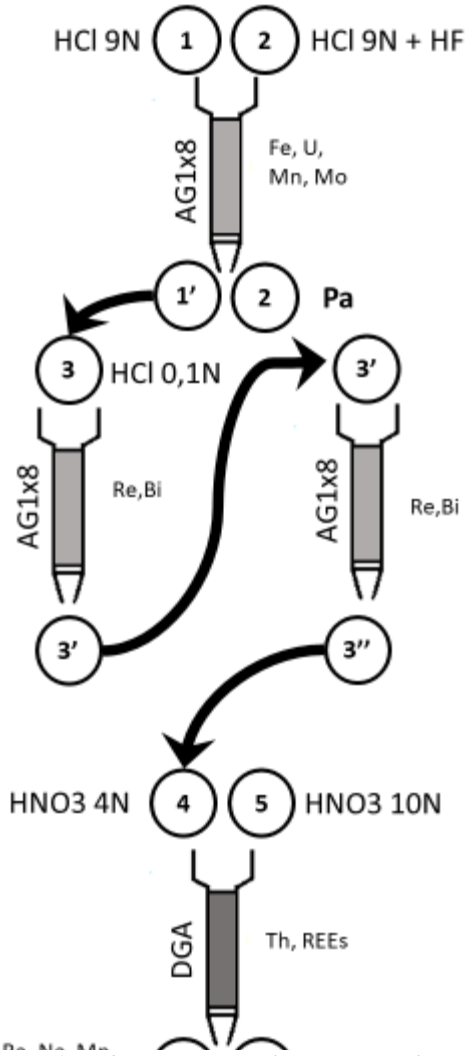


*Figure 1 : column sequence of actinium purification with element separation during the protocol. The column 2 is repeated to improve the rhenium removal*

198

199 To purify actinium from the Mn precipitate and potential interfering element, we used
200 several chromatographic columns, summed up in figure 1 and Tab. ES1. The first column
201 was filled with 2 mL of AG1x8 200-400 mesh and preconditioned with 9M HCl. After sample
202 loading, Th, Ra and Ac were eluted with 10mL HCl 9M, then Pa was eluted with 10 mL 9M
203 HCl + 0.1M HF, while most Mn stayed adsorbed on the resin. The Th-Ra-Ac fraction was
204 dried and dissolved in 0.1M HCl. The second column was added to remove Re, Bi, Pb, Mo
205 …, some of the most troublesome element that could interfere during mass spectrometry
206 analysis. It was filled with 2 mL of AG1X8, but preconditioned with 0.1M HCl. Th, Ac and
207 Ra were eluted directly in 0.1 M HCl while Re and Bi were kept on the resin. This step was
208 performed twice as preliminary tests had shown that a single column was not sufficient to
209 remove all the seawater Re. The resulting Ac-Th-Ra fraction was dried and dissolved in 4M
210 $HNO_3$. The last column was filled with 1 mL of TODGA resin 200-400 mesh, preconditioned
211 with 30 mL of 0.1M HCl and 20 mL of 4M $HNO_3$. After loading the sample, the radium
212 fraction was eluted with 15 mL of 4M $HNO_3$, together with Ba, Ca and Sr and the leftover of
213 Mn. Ac was eluted with 30 mL of 10M $HNO_3$. The last fraction, containing Th and REEs,
214 was eluted with 15 mL of 0.1M HCl. The Ac fraction was converted in 1mL of 1M $HNO_3$ +
215 0.013M HF and filtered at 0.4 µm to remove any resin grain before analysis by MC-ICPMS.

216 For seawater samples from the South China Sea (HYDROSED) samples, 4L of seawater were
217 subsampled to analyse $^{231}Pa$ and Th isotopes independently. The preparation protocol used
218 was the same as Gdaniec and al. (2018), except that co-precipitation was carried out with Mn
219 oxides like the Ac preparation protocol presented above. For the Southern Ocean seawater
220 samples (Bonus GoodHope), $^{231}Pa$ was extracted directly from the 9 L samples using the full
221 protocol (Fig. 1).

## 3. Mass spectrometry

The analyses were done on a ThermoScientific Neptune$^{plus}$ Multi-Collector Inductively Coupled Plasma Mass Spectrometer (MC-ICP-MS) equipped with a Jet interface, hosted at LSCE. An Aridus II and an Apex Omega HF were used as desolvating systems for Pa analysis (Gdaniec et al., 2018) and for Ac, respectively. Comparison of these two desolvating systems showed that they lead to the same sensitivity improvement (around $10^8$ cps/ppb, corresponding to an ion yield of 2%), but the signal was more stable with the Apex Ω HF system due to a better gas flow control which allows reducing uncertainties for samples analysis and the instrumental blank. The nebulizer had an uptake flow of 100 µL/min. To improve the stability of low level signals, we used the ion counters with the lowest dark noises. To reduce potential interferences and keep the background as low as possible, we used a sample introduction system (cones, probe, nebulizer, Apex Omega HF) specifically dedicated to Ac analyses. This introduction system was rinsed for at least 12h with 1M $HNO_3$ + 0.013M HF before the first analysis. The measurements were made in static mode, one ion counter by isotope, by counting 30 runs of 8.4s integration time. The mass calibration of the instrument and peak positioning were made with a solution prepared by diluting some $^{227}$Ac stock solution and adding $^{225}$Ra recovered from the milking (mass deviation between $^{225}$Ra and $^{225}$Ac = 0.0004 amu).

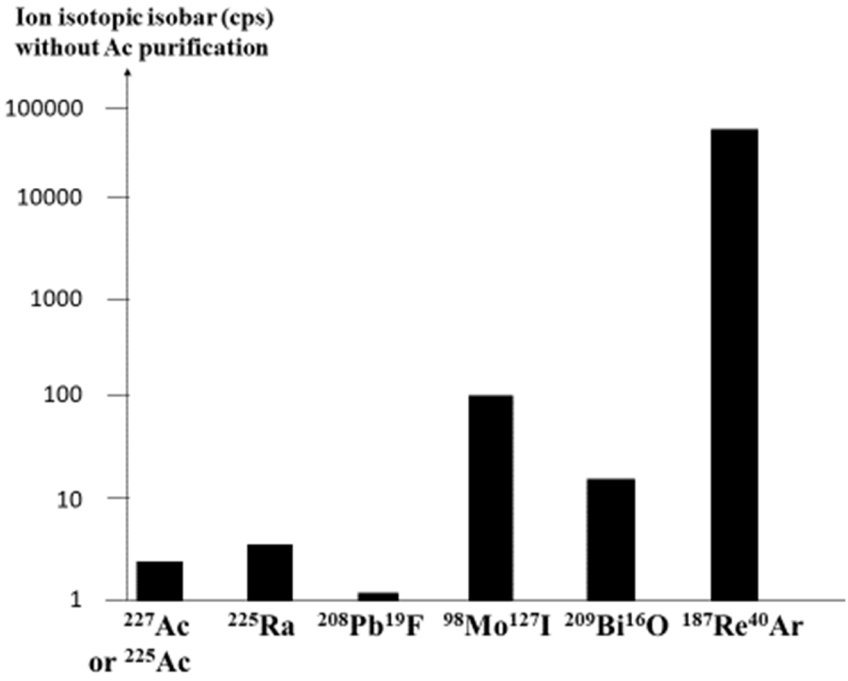


*Figure 2 : Expected signal on MC-ICPMS at mass 227 or mass 225 assuming a ratio 1:1 from actinium isotopes and the different interfering recombination from main elements brought by seawater matrix and by the reagents*

When measuring very low ion signals, it is necessary to consider possible interferences with polyatomic ions (Foster et al., 2004). Mass to charge ratios of $^{225}$Ac and $^{227}$Ac might potentially be interfered by isobaric interference made of mono or polyatomic ions (Fig. 2). The most obvious one was $^{225}$Ra from the spike. Several elements producing significant isobaric interferences if they are concentrated from the seawater samples were specifically removed during the chemical purification (Fig. 2): Bi ($^{209}$Bi$^{16}$O), Re ($^{185}$Re$^{40}$Ar and $^{187}$Re$^{40}$Ar), Pb ($^{208}$Pb$^{19}$F), Mo ($^{98}$Mo$^{127}$I), REE (although the precise nature of the ions was not determined, REE standard solution analysed at ppb level yielded peaks at mass 225 and 227). In spite of the cautions taken (use of a desolvator system, a nebulizer, tubing and cones dedicated to Ac isotopes only), some parasitic peaks were still observed close to mass 225 and 227 with count rates of 2 to 10 cps. These interferences were often observed even while the introduction system was rinsed with 1M $HNO_3$ + 0.01M HF. These peaks were lighter by ~ 0.17 amu compared to the actinium isotope

masses (Fig. 3). This is why, during Ac analysis, we did not carry out the measurement on the true $^{225}$Ac and $^{227}$Ac masses (225.0232 and 227.0278 amu), but we shifted to higher masses (around 225.12 and 227.12) to collect ions over the non-interfered part of the Ac peaks. It reduced the background level to ~0.2 counts per second, without Ac signal loss compared to the analysis at the peak centre.

The analysis was done in the low resolution of the Neptune (the mass resolution was $m/\Delta m \approx 500$ where $\Delta m$ is the peak width and the resolving power was $m/\Delta m \approx 1800$ where $\Delta m$ is the width of the peak side; Ireland, 2013), because at medium or high resolution, due to the ion transmission reduction, the sensitivity was too low to obtain sufficient counting statistics.

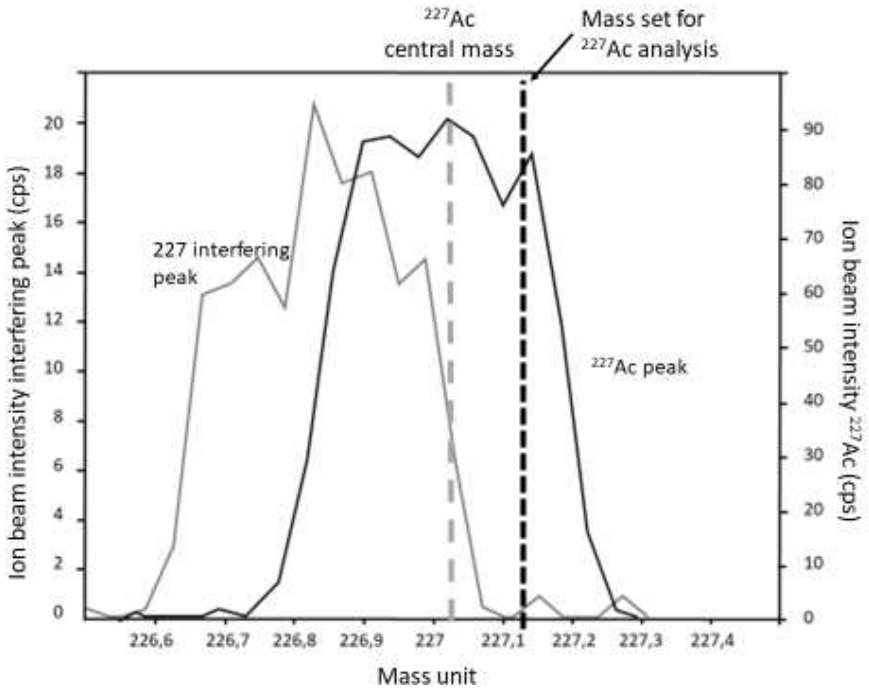


*Figure 3: $^{227}$Ac peak and its interfering peak close to m/z = 227. Composite figure showing the partial overlap between $^{227}$Ac (black) and the isobaric interfering peak (grey). The black dotted line at m/z= 227.12 is located where the $^{227}$Ac peak was measured while the grey dotted line is at m/z= 227.02, where is the $^{227}$Ac centre peak.*

## 3. Results

### 3.1. Standard analyses and calibration

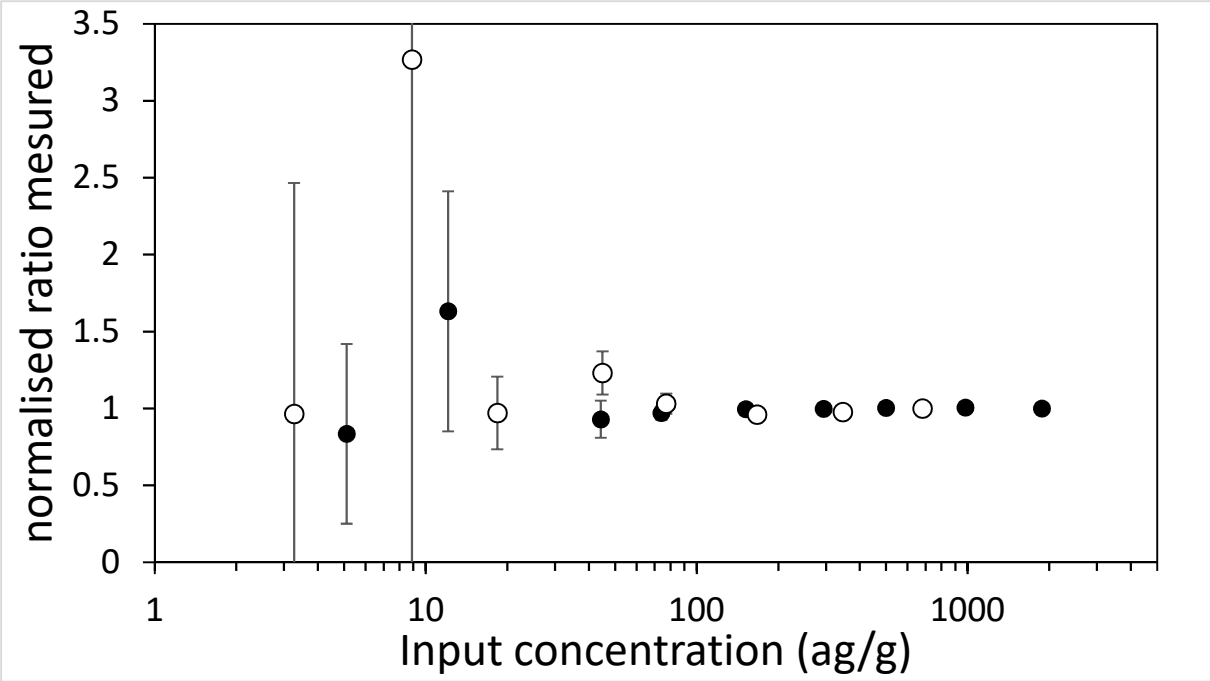


*Figure 4: Normalised ($^{225}Ac/^{227}Ac$) ratio measured by MC-ICPMS versus the Ac content for two series of successive dilutions of a spiked actinium solution (uncertainties $2\sigma_n$)*

A sensitivity test was made with successive dilutions of an Ac solution, with $^{225}Ac$ and $^{227}Ac$ at a ratio 1:1, from 2000 ag/g to 5 ag/g (Fig. 4). We used the ratio measured with the highest concentration input as a reference to normalisation of the measured ratios. When the concentration introduced in the instrument decreased, the measured ratio remained constant while the uncertainties grew significantly. For instance, the relative expanded uncertainty (confidence interval = 95%) is 30% with a concentration of 20 ag/g introduced into the instrument. These lowest concentrations correspond to a signal of ~1cps for each Ac isotopes, whereas a noise of 0.2 cps is typically measured for the acid blanks. The uncertainties of the most diluted solutions were dominated by the noise from the very low signal acquired by MC-ICPMS, while the uncertainties for the least diluted solution were dominated by the uncertainties on the $^{225}Ac$ spike concentration. The uncertainties were estimated through 20 runs of measurement and propagated by Monte Carlo through all the signal treatment and isotopic dilution calculation.

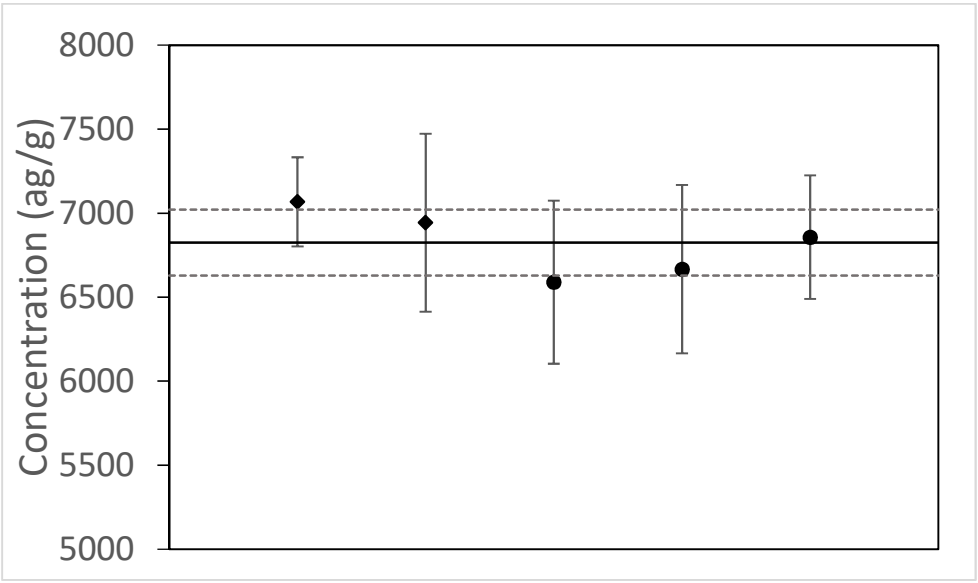


*Figure 5: Repeated measurements of the standard calibration solution, carried out in February 2019 (diamonds) and in October 2019 (circles). The concentration measured in February 2019 were corrected from the $^{227}$Ac decay to be compared with the October data. The solid line represents the average value of the all the measurements and the dotted lines the 95% confidence interval.*

The standard calibration was done twice in February 2019 and three time in October 2019. The concentrations measured in October 2019 were corrected from the $^{227}$Ac decay to be compared with the February data. The average concentration was at 6800 ± 200 ag/g ($2\sigma_n$) (Fig. 5).

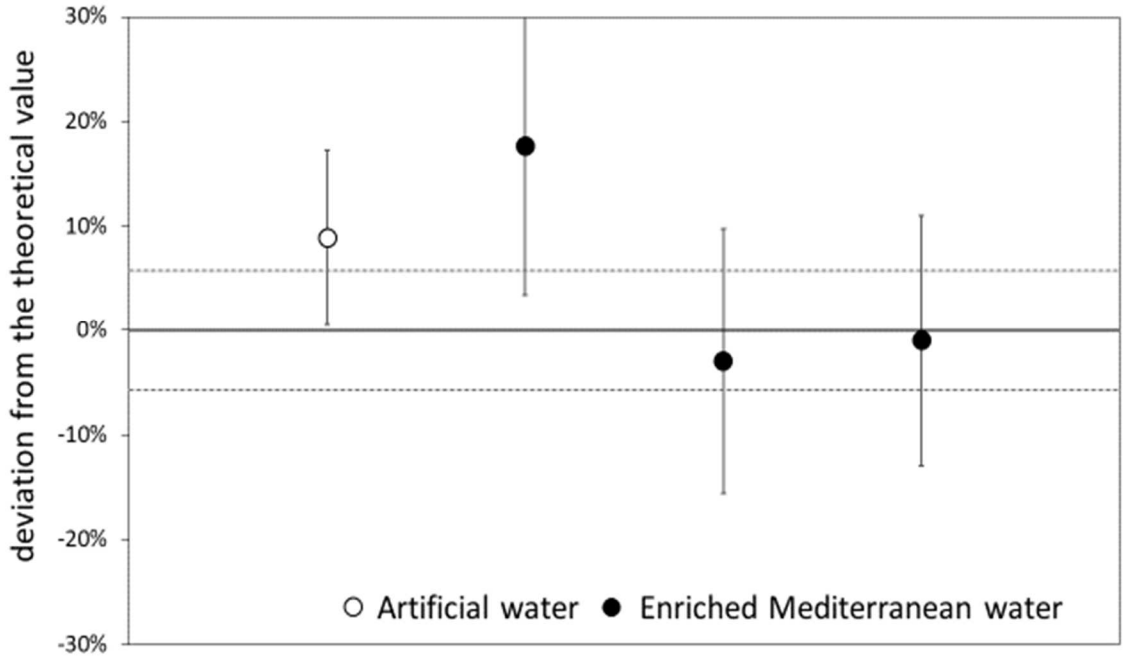


*Figure 6 : Deviation of the concentration measured against the concentration calculated from the dilution of our standard in artificial water (blank) and in Mediterranean seawater (black). The solid line represents the concentration of the home standard and the dotted lines the 95% confidence interval over the concentration of the home standard.*

The $^{227}$Ac concentrations in artificial seawaters and Mediterranean seawaters enriched in $^{227}$Ac from the stock solution were measured and compared to the calculated concentration. There is a good agreement between the theoretical concentration and the concentrations measured directly by MC-ICPMS (Fig. 6).

*Table 1: Actinium recovery yield for column chemistry and total protocol estimated from the signal intensity acquired on MC-ICPMS for different preparations*

| | Standard solution without | Column chemistry | Mn precipitation + Column | Mn precipitation |
|---|---|---|---|---|

| | chemistry | only | chemistry | |
|---|---|---|---|---|
| Signal intensity 29 L (cps) | 5.80 | 5.11 | 2.8 | |
| Yield 29 L | | 88% | 48 % | 55 % |
| Signal intensity 10 L (cps) | 16.2 | 14.7 | 12.86 | |
| Yield 10L | | 91% | 79 % | 87% |

317

318 The chemical yield was estimated for the different steps of the purification process
319 based on the intensity of the $^{225}$Ac signal measured by MC-ICPMS after different processing
320 (Table 1) during the seawater sample HS6 analyse batch (29 kg of seawater). The yield of the
321 ion exchange protocol was 88%. The full procedure yield was estimated to be ~ 48%.
322 Comparing the yield of the column chemistry (88%) and the full protocol suggests that the
323 precipitation yield on 30 L was ~ 0.48/0.88 = 55%. We also determined the Mn
324 preconcentration yield from 10 L of seawater sample and using the same amount of Mn as for
325 29 L of seawater. This yield was estimated to 87% by the ion counting comparison. The
326 improvement compared to the precipitation with 29 L is certainly due to the threefold increase
327 of the Mn/sample ratio. The Mn preconcentration yield was also performed by isotope
328 dilution on 10 L of artificial water and the same amount of Mn, the yield measured were 92%
329 and 98% that is in good agreement with the ion counting estimation.

330 Chemical blanks were triplicated for each analysis batch and the detection limit was
331 defined from these measurements. The blanks ranged from 4.8 ag to 8.5 ag with a standard
332 deviation of 2.5 ag. The detection limit of $^{227}$Ac was estimated at 7.5 ag of $^{227}$Ac (3 times the
333 blank standard deviation) introduced in the MC-ICPMS. For the HS6 samples, the detection
334 limit (LD) was 0.3 ag/kg for 30 L of seawater. For the “Bonus GoodHope” sample, the LD
335 was 0.8 ag/kg for 10L of seawater.

336

337 3.2. Water samples

338 Pa data are corrected from the ingrowth of $^{231}$Pa from the $^{235}$U decay and from the $^{231}$Pa decay
339 as follows:

340 $$N_{Pa}^{0} = e^{t\lambda_{Pa}} \times (N_{Pa}^{t} + \frac{\lambda_U}{\lambda_{Pa} - \lambda_U} \times N_U^0 \times \left(e^{-t\lambda_{Pa}} - e^{-t\lambda_U}\right))$$

341 With $N_{Pa}$ the atom concentration of $^{231}$Pa, at the sampling time (t = 0) and analysis time (t),
342 $N_U$ the atom concentration of $^{235}$U, estimated from the salinity of seawater (Owens et al.,
343 2011). $\lambda_{Pa}$ and $\lambda_U$ are the decay constant respectively for $^{231}$Pa and $^{235}$U, respectively.

344 The $^{227}$Ac concentration is corrected by considering the decay of $^{227}$Ac and its
345 ingrowth from $^{231}$Pa decay and the radioactive decay of $^{231}$Pa and its ingrowth from $^{235}$U
346 decay (that can be significant, especially in surface water) between the sampling time and the
347 analysis time (Bateman, 1910):

348 $$N_{Ac}^{0} = e^{t\lambda_{Ac}} \times (N_{Ac}^{t} - N_U^0 \times \lambda_{Pa}\lambda_U$$

349 $$\times \left( \frac{e^{-t\lambda_U}}{(\lambda_{Ac} - \lambda_U)(\lambda_{Pa} - \lambda_U)} + \frac{e^{-t\lambda_{Pa}}}{(\lambda_{Ac} - \lambda_{Pa})(\lambda_U - \lambda_{Pa})} \right.$$

350 $$\left. + \frac{e^{-t\lambda_{Ac}}}{(\lambda_{Pa} - \lambda_{Ac})(\lambda_U - \lambda_{Ac})} \right) - \frac{\lambda_{Pa}}{\lambda_{Ac} - \lambda_{Pa}} \times N_{Pa}^{0} \times \left(e^{-t\lambda_{Pa}} - e^{-t\lambda_{Ac}}\right))$$

351 With $N_{Ac}$ the atom concentration of $^{227}$Ac, at the sampling time (t = 0) and analysing time (t),
352 and $\lambda_{Ac}$ the constant decay of $^{227}$Ac.

353 The Ac concentration supported by the Pa decay in ag/kg (Fig. 7.a) is calculated from Pa
354 (conversion factor around 0.66), with $M_{Ac}$ the molar mass of $^{227}$Ac and $M_{Pa}$ the molar mass of
355 $^{231}$Pa:

356 $$Ac_{supported}\,(ag/kg) = Pa\,(fg/kg) \times \frac{M_{Ac}}{M_{Pa}} \times \frac{\lambda_{Pa}}{\lambda_{Ac}} \times 10^3$$

357 For continental waters, $^{227}$Ac concentrations of 4.1 ± 1.3 ag/kg and 6.1 ± 1.7 ag/kg
358 were measured in 20 L and 35 L water samples from Vienne River, respectively (Table 2). By
359 contrast, a $^{227}$Ac concentration as high as 2640 ±260 ag/kg was measured in a water sample
360 from the Rusquec pond, in Britany (France), characterized by a high environmental Ac
361 background level.

362 $^{227}$Ac concentrations measured for seawater samples from HS6 station ranged from
363 below the detection limit (0.5 ag/kg) to 3.9 ± 1.0 ag/kg at 1800 m (Fig. 7.a), followed by a
364 sharp decrease at 2400 m (2.0 ± 0.5 ag/kg) and then an increase at the seafloor (3.3 ± 0.7
365 ag/kg). The concentration of $^{231}$Pa was also measured at this station, allowing to calculate the
366 concentration of $^{227}Ac_{supported}$. The $^{227}Ac_{supported}$ was 0.23 ag/kg in surface waters, increased to
367 1.5 ag/kg at a depth of 2000 m and then decreased in deeper waters. This profile is similar to
368 the $^{230}$Th profile (Fig. 7.b), with an increase from 1 fg/kg in surface waters to 13 fg/kg at 1800
369 m and a lower and roughly constant concentration of 7 fg/kg in deeper water.

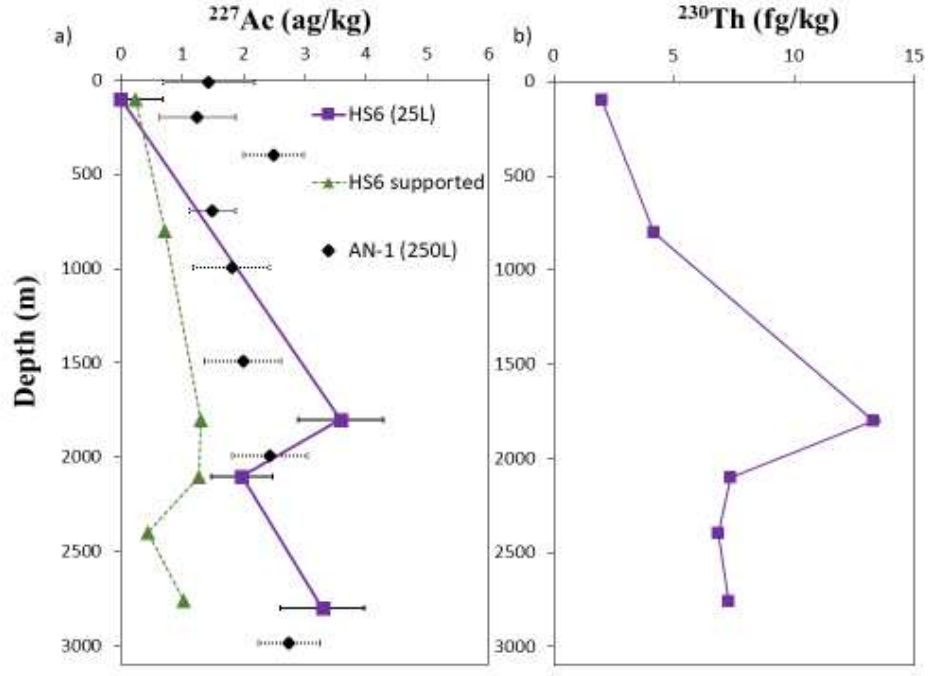

370

371 *Figure 7 : (a)$^{227}$Ac concentration profile in China Sea (purple square), with the actinium concentration supported by the Pa*
372 *decay (green triangle), and the concentration measured in west Pacific (black diamand) by Nozaki (1990), (b) $^{230}$Th profile at*
373 *the station HS6 in the China Sea. All the uncertainties are expressed at $2\sigma_n$*

374

375

376 *Table 2 : $^{227}$Ac concentrations measured in environmental water. All the concentrations are corrected from the decay*
377 *between sampling time and analysis time.*

| Sample | sample mass (kg) | $^{227}$Ac (ag/kg) ($2\sigma_n$ uncertainties) | $^{231}$Pa (fg/kg) ($2\sigma_n$ uncertainties) |
|---|---|---|---|
| *Seawater* | | | |
| Hydrosed | | | |
| HS6 100 m | 29 | 0.1 ± 0.7 (<LD) | 0.36 ± 0.03 |
| HS6 800 m | 4 | | 1.08 ± 0.06 |
| HS6 1800 m | 29 | 3.9 ± 1.0 | 1.99 ± 0.09 |
| HS6 2100 m | 29 | 2.0 ± 0.5 | 1.93 ± 0.07 |
| HS6 2400 m | 4 | | 0.67 ± 0.04 |
| HS6 2760 m | 29 | 3.3 ± 0.7 | 1.56 ± 0.05 |
| | | | |
| Bonus GoodHope | | | |
| Super V 134 m | 9.4 | 4.1 ± 1.1 | 0.42 ± 0.04 |
| Super V 247 m | 10.2 | 3.9 ± 1.8 | 0.98 ±0.05 |
| Super V 396 m | 9.4 | 6.7 ± 1.3 | 1.84 ± 0.03 |
| Super V 692 m | 10.6 | 5.1 ± 1.6 | 1.90 ± 0.09 |
| Super V 1185 m | 8.8 | 5.2 ± 2.0 | 2.29 ± 0.11 |
| Super V 1776 m | 9.1 | 6.3 ± 1.2 | 2.39 ± 0.06 |
| Super V 2462 m | 9.0 | 7.8 ± 1.3 | 2.12 ± 0.08 |
| Super V 3848 m | 9.5 | 9.9 ± 1.6 | 3.45 ± 0.06 |
| | | | |
| *Continental water* | | | |
| Vienne river | 20 | 6.1 ± 1.7 | |
| Vienne river | 35 | 4.1 ± 1.3 | |
| Rusquec pond | 1 | 2640 ± 261 | |

378

379

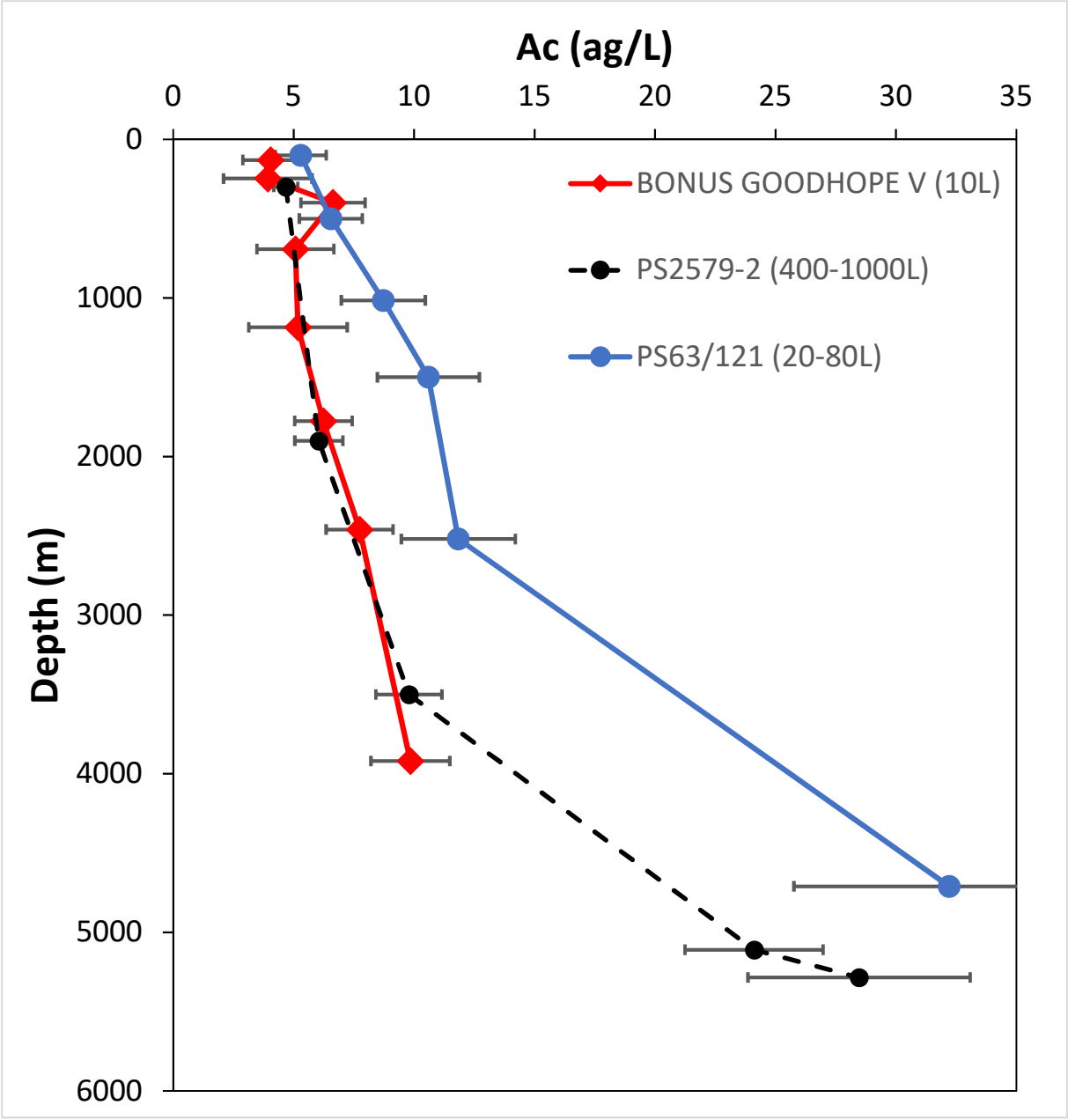


*Figure 8 : Seawater $^{227}$Ac profiles in Weddell Gyre, at station Super V from Bonus GoodHope cruise, measured by mass spectrometry (red diamonds) and at station PS2579-2 (Geibert, 2002) (black dot) and PS63-121 measured by alpha-spectrometry (Geibert and Vöge, 2008) (blue dots). All uncertainties are expressed at 2$\sigma_n$*

The $^{227}$Ac concentrations measured in Bonus GoodHope samples from the Weddell gyre increase steadily with depth, from 4.1 ± 1.1 ag/kg at 136 m, to 9.9 ± 1.6 ag/kg at 3848 m (Fig. 8). The average uncertainty is around 20% (expressed as 2$\sigma_n$). Samples at 247 m, 692 m and 1185 m have larger uncertainties because their analysis had to be delayed by more than 2

weeks due to a breakdown of the MC-ICPMS, leading to a loss of more 50% of the $^{225}$Ac spike during this period. The $^{227}$Ac profile is in good agreement with the data from the Weddell Gyre (Geibert et al., 2002; Geibert and Vöge, 2008). We did not have a sample from just above the seafloor at 3932 m to observe the expected large increase in $^{227}$Ac concentration due to diffusion from the sediment.

## 4. Discussion

### 4.1. ID-MC-ICPMS method assessment

The main challenge of this protocol for $^{227}$Ac analysis in natural waters is to remove every element which could produce isobaric interferences with $^{227}$Ac or $^{225}$Ac (Fig. 2). First, we identified likely interferences which consist of isobaric recombination between elements from the sample and from the matrix ($^{40}$Ar, $^{16}$O, $^{14}$N, $^{19}$F, $^{1}$H) in the plasma, in order to remove problematic elements during the chromatographic purification. Most of the interfering peaks were removed, but some remained. Then, we tried to identify the remaining interferences with two different methods. First, we compared mass scans from mass 215 to mass 231 with the isotopic abundance patterns of elements which may constitute the poly-atomic ions. This allowed us to identify, during a particular run, the MoI recombination that had not been considered before. The second method consisted in the precise determination of the masses of the interfering peaks. This was done by averaging the masses at half-maximum peak height of the interfering peaks. For mass 227, the $^{227}$Ac atomic mass is 227.028, while the atomic mass of the interfering peak was around 226.83. Interestingly, the atomic mass of $^{187}$Re$^{40}$Ar is 226.92 amu, which is significantly higher than the measured mass of the interference, discarding Re as the cause of the interference. Some atomic combination could have similar masses like $^{147}$Sm$^{40}$Ar$_2$ (226.840) but the mass scan around the 227 mass did not show the

413 pattern that would be expected with this element. Moreover, there was no signal at the masses
414 around the 225 and 227 and only 200 cps were recorded at m/z of $^{187}$Re, which is too low to
415 expect a significant interference from ReAr. Therefore, as of now the nature of these
416 interferences at masses 225 and 227 remains undetermined. Nevertheless, we took advantage
417 of this mass offset to analyse $^{225}$Ac and $^{227}$Ac peaks on the high side of these peaks at masses
418 where the interfering ions can be neglected (Fig. 3).

419 In addition, we performed different tests to assess the robustness of our new $^{227}$Ac
420 analysis method. First, we tested the reproducibility of the measurement by MC-ICPMS by
421 the analyses of successive dilutions of a single solution (Fig. 2), carried out several times with
422 a consistent result whatever the dilution and the dates of these experiments. This demonstrates
423 that our settings for the MC-ICPMS is suitable to analyse low level signals of Ac isotopes and
424 the statistical uncertainty estimated allow us to expect good reliability for the seawater
425 concentrations. Most published $^{227}$Ac measurements (RaDeCC and alpha spectrometry) in
426 seawater are given with a 1 $\sigma_n$ relative standard uncertainties around 10-20%, so we choose a
427 $2\sigma_n$ relative expanded uncertainty of 20% as suitable uncertainty for our measurements by
428 MC-ICPMS. For smaller signals, uncertainties of the MC-ICPMS measurements increase
429 significantly (Fig. 4). The required concentration of the solution injected into the plasma to
430 have a measurement with a statistical relative expanded uncertainty of 20% was around 20
431 ag/g, corresponding to a count rate of around 1 cps for $^{225}$Ac and $^{227}$Ac (Fig. 4). These limits
432 allow us to make reliable measurements with 10 L samples with $^{227}$Ac concentrations of ~ 2
433 ag/kg with a detection limit around 0.7 ag/kg estimated from our chemical blank.

434 Then, we tested the robustness of the chemical process by duplicating some
435 experiments. The calibration of our $^{227}$Ac standard against a $^{229}$Th spike at secular equilibrium
436 with $^{225}$Ac was repeated for different periods, in different batches of samples giving consistent

437 results (Fig. 4). Similarly, the replication of the measurements of artificial and doped
438 seawaters processed through the whole chemistry gave consistent results in good agreement
439 with concentrations prepared by dilution of the $^{227}$Ac stock solution (Fig. 6). The
440 reproducibility of the results from the above experiments make us very confident in the
441 successful application of our protocol for analysis of natural waters. This relies on the use of
442 isotope dilution that removes uncertainties on the Mn coprecipitation and purification yields.

443 The first samples analysed were from South China Sea, near the Luzon strait. The
444 surface concentration of $^{227}$Ac was below our detection limit (10 ag from 30L of sample) for
445 $^{227}$Ac. Within analytical uncertainties, this result is not significantly different from the
446 concentration of $^{227}$Ac supported by the $^{231}$Pa decay (HS6-100 m : $^{227}Ac_{supported}$= 0.24 ag/kg)
447 as expected for surface water. For the deep samples, $^{227}$Ac concentrations are generally
448 consistent with the signature of Pacific Deep Water (PDW) (Nozaki et al., 1990). However,
449 the $^{227}$Ac profile seems affected by scavenging below the Luzon strait (highlighted by the
450 sharp decrease of the $^{230}$Th concentrations below 1800 m) and diffusion from the seafloor
451 (suggested by the increase between the concentration at 2400 m and 2700 m) (Fig. 7.b). We
452 also analysed waters from the Weddell Gyre (Fig. 8). Our measurements are in good
453 agreement with previously published data (Geibert et al., 2002, 2008), despite the use of only
454 10 L of seawater, collected 12 years before analysis. One of the unexpected results obtained
455 by Geibert was the relatively high concentration $^{227}$Ac in surface water in the Weddell Gyre, a
456 feature that we confirm with ID-MC-ICPMS.

457 To our knowledge, there is no river data to compare the $^{227}$Ac concentration measured
458 in the Vienne River. Nevertheless, the 2 analyses of the same water sample agree within
459 uncertainties. Despite concentrations similar to seawater, the uncertainties are still 20-25%
460 ($2\sigma_n$), probably due to a lower precipitation yield because the filters needed to be changed
461 several times during the co precipitation step.

462 Overall, these different experiments strengthen our trust in the reliability of the $^{227}$Ac
463 concentration measurement by ID-MC-ICPMS for seawater and freshwater samples.

464

465 4.2. Comparison with other methods

466 The different tests that we have performed in this study give a $^{227}$Ac detection limit of
467 around 10 ag, with a 2 $\sigma_n$ uncertainty of ~ 20-25%. This detection limit allows us to measure
468 sample with around 10L, that size is comparable to the volume of the Niskin bottle generally
469 used during oceanographic cruise. This is a very significant improvement compared to
470 methods used until now. The method based on measurement by alpha-spectrometry used by
471 Nozaki allowed to measurements of samples with $^{227}$Ac concentrations of ~1 ag/kg but
472 required around 250 L (Nozaki, 1993). This method had a good reliability for the
473 concentration measurement, thanks to the measurement of $^{227}$Th which is at equilibrium with
474 $^{227}$Ac, after 100 days of equilibration, spiked with $^{230}$Th. However, the yield of the
475 preconcentration on Mn fibers for Ac was not well-known and is only assumed to be equal to
476 the extraction efficiency of Ra.

477 Alpha spectrometry was also used for analysis of samples from the Weddell Gyre
478 (Geibert et al., 2002; Geibert and Vöge, 2008). $^{227}$Ac in the Weddell Gyre is more
479 concentrated than in the Pacific Ocean, so only 20 to 80L of seawater were required. The
480 implemented method was the same as the one of Nozaki, but spiking with $^{225}$Ac was
481 performed before the preconcentration step to have a better estimate of the yield and to
482 decrease the total uncertainties on the measurement. The lowest volume (20 L) was used to
483 analyse the most concentrated sample (32 ag/kg with a 2$\sigma$ uncertainty of 18%). This must be
484 compared with our results from the HYDROSED profile for which 29 L of seawater were
485 used to analyse concentrations of the order of 3 ag/kg (with a 2 $\sigma_n$ uncertainty of 25%).

The RaDeCC method requires pumping over 1000L of seawater through a Mn-Cartridge to perform measurement at around 0.4 ag/kg with a 2σ uncertainty of ± 34% (Le Roy et al., 2019) which is less precise and requires much larger volume than our method. This protocol is derived from the measurement of Ra isotopes with RaDeCC (scintillation cells) by measuring the activity of $^{223}$Ra and $^{219}$Rn at the equilibrium with $^{227}$Ac after at least 3 months of equilibration (Shaw and Moore, 2002). With this method, the yield of Ac recovery on Mn-cartridge yield ranged from 31 to 78% with a mean value (47 ±12 %) that is arbitrarily used for all the low concentration samples for which the yield could not be directly determined. Keeping in mind that RaDeCC analysis requires 100 times more water than ID-MC-ICPMS, it has a lower detection limit (detection limit estimated around 400 ag or 0.1 ag/kg, if the yield on the Mn cartridge is taken into account).

At last, it is necessary to measure the dissolved $^{231}$Pa to calculate the unsupported $^{227}$Ac, which is the parameter for interpreting $^{227}$Ac data in seawater. Our method by ID-MC-ICPMS allows to measure the two elements from the same water sample. $^{231}$Pa is adsorbed on Mn oxide (Rutgers van der Loeff and Moore, 1999) and is purified during the first anion exchange chromatography (Gdaniec et al., 2018). Other tracers can be recovered during the chemical process, i.e. a Ra fraction with alkaline earth elements that could be used for $^{226}$Ra and $^{228}$Ra analyse, and a fraction with the Th and REEs that could be used for the measurement of the isotopic composition of Nd and relative abundance of the different REEs. Pa cannot be analysed with the RaDeCC protocol, but it can be measured by alpha spectrometry.

## 5. Conclusion

510 This study presented the first analytical protocol for measurement of the dissolved $^{227}$Ac in
511 natural waters by means of a thorough chemical purification-concentration procedure, MC-
512 ICPMS and quantification of $^{227}$Ac by isotopic dilution with $^{225}$Ac. This method has an
513 improved sensitivity and lower uncertainties than the methods based on nuclear counting. It
514 allows significantly reducing the sample size to the volume of common sampling bottle (i.e.
515 10-30 L) and it will be particularly useful to analyse pore water or hydrothermal fluids
516 (Geibert et al, 2008, Kipp et al, 2015). This method also provides purification-concentration
517 of other oceanic tracers like $^{231}$Pa, $^{226}$Ra, REEs or $\varepsilon_{Nd}$. Some improvements are still needed to
518 reduce the interferences on MC-ICPMS and to carry out inter-calibration of standards to
519 strengthen the reliability of the Ac measurement. This new method paves the way for the
520 analysis of $^{227}$Ac by laboratories which are not equipped with nuclear counting systems, but
521 which are already able to measure $^{231}$Pa and $^{230}$Th by MC-ICPMS. This will allow a rapid
522 growth of the use of $^{227}$Ac as an ocean tracer.

523

524 Acknowledgement

525 The authors would like to thank Edwige Pons-Branchu, Eric Douville, Lorna Foliot for
526 advices on the chemistry and mass spectrometry development and Nadine Laborde and
527 François Thil for the opportunist sampling of Vienne sample. Philippe Bonté kindly provided
528 the “mare du Rusquec” sample. We acknowledge all the sampling team on board the Marion
529 Dufresne during the HYDROSED cruise and Bonus GoodHope cruise. We thank Fabien
530 Pointurier for his thorough review of the manuscript. This work benefited from the French
531 government support managed by the ANR under the “Investissement d’avenir” programme
532 [ANR-11-IDEX-0004-17-EURE-0006], supported by the COMUE Paris Saclay University.

533 This work was also supported by the French National program LEFE (Les Enveloppes Fluides
534 et l'Environnement).

## References


Bateman, H., 1910. Solution of a system of differential equations occurring in the theory of radioactive transformations. Proc. Cambridge Philos. Soc. 15, 423–427.

Bojanowski, R., Holm, E., Whitehead, N.E., 1987. Determination of $^{227}$Ac in environmental samples by ion-exchange and alpha spectrometry. J. Radioanal. Nucl. Chem. 115, 23–37. https://doi.org/10.1007/BF02041973

Foster, D. A., Staubwasser, M., & Henderson, G. M.,2004. Ra-226 and Ba concentrations in the Ross Sea measured with multicollector ICP mass spectrometry. Marine Chemistry, 87, 59-71.

Gdaniec, S., Roy-Barman, M., Foliot, L., Thil, F., Dapoigny, A., Burckel, P., Garcia-Orellana, J., Masqué, P., Mörth, C.-M., Andersson, P.S., 2018. Thorium and protactinium isotopes as tracers of marine particle fluxes and deep water circulation in the Mediterranean Sea. Mar. Chem. 199, 12–23. https://doi.org/10.1016/j.marchem.2017.12.002

Gdaniec, S., Roy-Barman, M., Levier, M., Valk, O., van der Loeff, M.R., Foliot, L., Dapoigny, A., Missiaen, L., Mörth, C.-M., Andersson, P.S., 2020. $^{231}$Pa and $^{230}$Th in the Arctic Ocean: Implications for boundary scavenging and $^{231}$Pa $^{230}$Th fractionation in the Eurasian Basin. Chem. Geol. 532, 119380. https://doi.org/10.1016/j.chemgeo.2019.119380

Geibert, W., 2015. Assessment criteria for radionuclides in Geotraces IDP2017.

Geibert, W., Rutgers van der Loeff, M.M., Hanfland, C., Dauelsberg, H.-J., 2002. Actinium-227 as a deep-sea tracer: sources, distribution and applications. Earth Planet. Sci. Lett. 198, 147–165. https://doi.org/10.1016/S0012-821X(02)00512-5

Geibert, W., Charette, M., Kim, G., Moore, W. S., Street, J., Young, M., Paytan, A., 2008. The release of dissolved actinium to the ocean: a global comparison of different end-members. Marine chemistry, 109, 409-420.

Geibert, W., Vöge, I., 2008. Progress in the determination of $^{227}$Ac in sea water. Mar. Chem. 109, 238–249. https://doi.org/10.1016/j.marchem.2007.07.012

Ghaleb, B., Pons-Branchu, E., Deschamps, P., 2004. Improved method for radium extraction from environmental samples and its analysis by thermal ionization mass spectrometry. J. Anal. At. Spectrom. 19, 906. https://doi.org/10.1039/b402237h

Ireland, T. R., 2013. Recent developments in isotope-ratio mass spectrometry for geochemistry and cosmochemistry. Review of Scientific Instruments 84, 011101.

Kayzar, T.M., Williams, R.W., 2015. Developing $^{226}$Ra and $^{227}$Ac age-dating techniques for nuclear forensics to gain insight from concordant and non-concordant radiochronometers. J. Radioanal. Nucl. Chem. 307. https://doi.org/10.1007/s10967-015-4435-4

Kipp, L. E., Charette, M. A., Hammond, D. E., Moore, W. S., 2015. Hydrothermal vents: A previously unrecognized source of actinium-227 to the deep ocean. Marine Chemistry, 177, 583-590.

Komura, K., Yznamoto, M., Ueno, K., 1990. Abundance of Low-energy gamma rays in the decay of $^{238}$U,$^{234}$U, $^{227}$Ac, $^{226}$Ra and $^{214}$Pb. Nucl. Instrum. Methods Phys. Res. 295, 461–465.

Le Roy, E., Sanial, V., Lacan, F., van Beek, P., Souhaut, M., Charette, M.A., Henderson, P.B., 2019. Insight into the measurement of dissolved $^{227}$Ac in seawater using radium delayed coincidence counter. Mar. Chem. 212, 64–73. https://doi.org/10.1016/j.marchem.2019.04.002

Marinov, G.M., Marinova, A.P., Medvedev, D.V., Dadakhanov, J.A., Milanova, M.M., Happel, S., Radchenko, V.I., Filosofov, D.V., 2016. Determination of distribution

coefficients (Kd) of various radionuclides on UTEVA resin. Radiochim. Acta 104. https://doi.org/10.1515/ract-2016-2582
Nozaki, Y., 1993. Actinium-227: A Steady State Tracer for the Deep-sea Basin-wide Circulation and Mixing Studies, in: Teramoto, T. (Ed.), Elsevier Oceanography Series, Deep Ocean Circulation. Elsevier, pp. 139–156. https://doi.org/10.1016/S0422-9894(08)71323-0
Nozaki, Y., 1984. Excess $^{227}$Ac in deep ocean water. Nature 310, 486–488. https://doi.org/10.1038/310486a0
Nozaki, Y., Yamada, M., Nikaido, H., 1990. The marine geochemistry of actinium-227: Evidence for its migration through sediment pore water. Geophys. Res. Lett. 17, 1933–1936. https://doi.org/10.1029/GL017i011p01933
Owens, S.A., Buesseler, K.O., Sims, K.W.W., 2011. Re-evaluating the $^{238}$U-salinity relationship in seawater: Implications for the $^{238}$U–$^{234}$Th disequilibrium method. Mar. Chem. 127, 31–39. https://doi.org/10.1016/j.marchem.2011.07.005
Pommé, S., Marouli, M., Suliman, G., Dikmen, H., Van Ammel, R., Jobbágy, V., Dirican, A., Stroh, H., Paepen, J., Bruchertseifer, F., Apostolidis, C., Morgenstern, A., 2012. Measurement of the $^{225}$Ac half-life. Appl. Radiat. Isot. 70, 2608–2614. https://doi.org/10.1016/j.apradiso.2012.07.014
Pourmand, A., Dauphas, N., 2010. Distribution coefficients of 60 elements on TODGA resin: Application to Ca, Lu, Hf, U and Th isotope geochemistry. Talanta 81, 741–753. https://doi.org/10.1016/j.talanta.2010.01.008
Radchenko, V., Engle, J.W., Wilson, J.J., Maassen, J.R., Nortier, F.M., Taylor, W.A., Birnbaum, E.R., Hudston, L.A., John, K.D., Fassbender, M.E., 2015. Application of ion exchange and extraction chromatography to the separation of actinium from proton-irradiated thorium metal for analytical purposes. J. Chromatogr. A 1380, 55–63. https://doi.org/10.1016/j.chroma.2014.12.045
Roy-Barman, M., Folio, L., Douville, E., Leblond, N., Gazeau, F., Bressac, M., Wagener, T., Ridame, C., Desboeufs, K., Guieu, C., 2020. Contrasted release of insoluble elements (Fe, Al, REE, Th, Pa)after dust deposition in seawater: a tank experiment approach (preprint). Biogeochemistry: Open Ocean. https://doi.org/10.5194/bg-2020-247
Roy-Barman, M., Thil, F., Bordier, L., Dapoigny, A., Foliot, L., Ayrault, S., Lacan, F., Jeandel, C., Pradoux, C., Garcia-Solsona, E., 2019. Thorium isotopes in the Southeast Atlantic Ocean: Tracking scavenging during water mass mixing along neutral density surfaces. Deep Sea Res. Part Oceanogr. Res. Pap. 149, 103042. https://doi.org/10.1016/j.dsr.2019.05.002
Rutgers van der Loeff, M., Moore, W.S., 1999. Determination of natural radioactive tracers., in: Methods of Seawater Analysis. pp. 365–397.
Shaw, T.J., Moore, W.S., 2002. Analysis of $^{227}$Ac in seawater by delayed coincidence counting. Mar. Chem. 78, 197–203. https://doi.org/10.1016/S0304-4203(02)00022-1
Varga, Z., Nicholl, A., Mayer, K., 2014. Determination of the Th 229 half-life. Phys. Rev. C 89. https://doi.org/10.1103/PhysRevC.89.064310

628 Electronic supplement: Table. ES1: Elution table of chromatographic resin

| 1st column | | AG1x8 | 2mL |
|---|---|---|---|
| Wash | 9M HCl + 0.013M HF | | 10mL |
| | 9M HCl | | 10mL |
| | MQ | | 10mL |
| Conditioning | 9M HCl | | |
| Sample | | | 2mL |
| Th/Ac/Ra elution | 9M HCl | | 10 mL |
| Pa elution | 9M HCl + 0.013M HF | | 10mL |
| | | | |
| 2nd and 3rd column | | AG1x8 | 2mL |
| Wash | 0.1M HCl | | 10mL |
| conditioning | 0.1M HCl | | 10mL |
| Sample | | | 2mL |
| Th/Ac/Ra elution | 0.1M HCl | | 10 mL |
| | | | |
| 4th column | | TODGA | 1mL |
| Wash | 0.1M HCl | | 20mL |
| | MQ | | 10mL |
| Conditioning | 4M $HNO_3$ | | 15mL |
| Sample | | | 2mL |
| Ra Elution | 4M $HNO_3$ | | 15mL |
| Ac Elution | 10M $HNO_3$ | | 30mL |
| Th/REEs Elution | 0.1M HCl | | 15mL |

629